Journal of Chemical Health Risks

www.jchr.org

JCHR (2023) 13(6), 2706-2720 | ISSN:2251-6727

Molecular Docking, Pharmacophore Modeling and ADMET Profiling Study of Some Bioactive Phytochemicals from *Indigofera Tinctoria* as Potential Ppar$_{\upsilon}$ Inhibitors for the Treatment of Diabetes: An In-Silico Study

Maya Yadav[1*], Raj Kumar Singh Yadav[2]

[1,2]Assistant Professor, Department of Botany, Dr. Shyama Prasad Mukherjee Govt. Degree College, Bhadohi. UP, India-221401

(Received: 07 October 2023 Revised: 12 November Accepted: 06 December)

KEYWORDS
Molecular docking, Pharmacophore modeling, ADMET profiling, Bioactive phytochemicals, PPARϒ inhibitors.

ABSTRACT:

In the pursuit of effective therapeutic strategies for diabetes mellitus (DM), peroxisome proliferator-activated receptor- PPARγ agonists have emerged as promising oral antidiabetic medications. However, the prevalence of adverse effects associated with many existing medications underscores the need for novel and safer alternatives. PPARγ, a key regulator of glucose and lipid homeostasis, is the target receptor for thiazolidinediones, a synthetic class of anti-diabetic medications. Given its pivotal role in the pathogenesis of Type II diabetes mellitus, drug discovery efforts have intensified to identify new compounds targeting PPARγ. This study employs a multi-faceted approach, integrating pharmacophore analysis, pharmacokinetic/toxicity evaluation, and in-silico molecular docking, to investigate the antidiabetic potential of phytoconstituents derived from Indigofera tinctoria (I. tinctoria) as potential PPARγ agonists. Molecular docking analysis of 21 selected phytoconstituents from I. tinctoria reveals that 18 exhibit superior binding affinity ($\Delta G \geq -6.9$ K cal/mol) and remarkably low inhibition constants ($Ki \leq 0.35$ μM) compared to established thiazolidinediones—Pioglitazone and Rosiglitazone ($\Delta G \leq 6.9$ K cal/mol, $Ki \geq 8.74$ μM).Among the top-performing compounds, namely Pseudosemiglabrin, Dehydrodeguelin, Apigenin, Tephrosin, Indirubin, and Indigo, further analysis through pharmacophore/ADMET profiling confirms their drug-likeness properties. These compounds adhere to Lipinski's Rule of 5, demonstrating favorable drug-like characteristics and exhibiting good oral bioavailability, as illustrated in the bioavailability radar. The findings suggest that naturally derived phytochemicals from I. tinctoria, particularly the identified compounds, hold promise as potential PPARγ agonists. These compounds, exhibiting robust in-silico characteristics, merit further experimental validation and may represent safer and more effective candidates for the development of novel antidiabetic agents.

1.0 Introduction:

Diabetes melitus (DM) is a chronic metabolic disease characterized by hyperglycemia, insulin resistance, and glucose tolerance. The distinctive features of DM encompass elevated blood glucose levels during fasting and postprandial periods, arising from compromised insulin secretion, action or both [1]. Presently, a staggering 463 million adults worldwide grapple with diabetes and projections for 2030 and 2045 anticipate a rise to 578 million and 700 million individuals [2], [3]. Notably, diabetes ranks among the top ten global causes of death [4]. The disease manifests in three forms: Type I diabetes (insulin-dependent), Type II diabetes (non-insulin-dependent) and gestational diabetes. Type II diabetes (T2DM) accounts for 90–95% of cases, representing the most prevalent form of the disease [5]. Characterized by insulin resistance, T2DM leads to hyperglycemia, subsequently causing glucotoxicity and long-term complications including both non-vascular (such as infections, gastroparesis, skin changes) and vascular issues (peripheral and coronary arterydiseases, cerebrovascular, and retinopathy) [1]. Current management strategies involve insulin injections and oral hypoglycemic medications such as insulin secretagogues, incretin agonists, insulin sensitizers, dipeptidyl peptidase-4 inhibitors, and α-glucosidase inhibitors. These approaches aim to achieve controlled blood glucose level: however, challenges arise from the accessibility, affordability and documented side effects of these treatments, including lactic acidosis, gastrointestinal distress, and hypoglycemia [6]–[8]. As the diabetic population continues to grow, the need for

Journal of Chemical Health Risks

www.jchr.org

JCHR (2023) 13(6), 2706-2720 | ISSN:2251-6727

safer and more effective therapeutic alternatives become increasingly imperative.

The exploration of antiviral effects against SARS-Cov-2 from phytochemicals found in various medicinal plants has been a subject of extensive research during the COVID-19 period [9]–[16]. Additionally, the investigation of medicinal activities, including hypercholesterolemia Inhibitory activity of *Withania coagulans* and the antitumor constituents, sidrin and sidroside, from *Zizyphus spina-christi* compounds, has further diversified the potential applications of these plants [17], [18]. This growing body of knowledge has spurred increased interest in utilizing medicinal plants, renowned for their diverse pharmacological and biological activities for the management and treatment of diabetes [19]–[25]. One such highly sought- after antidiabetic plant is *Indigofera tinctoria (I. tinctoria)*, a shrub belonging to the Fabaceae family. *I. tinctoria* has a long history of use in Chinese and Indian medicines addressing various conditions such as liver disorders, heart palpitations, and constipation [26]. Notably, its flavanoidal fraction demonstrates antiproliferative activity and its aqueous extract exhibits antioxidant activities, neuroprotective effects, and immunoprotevtive role [27]–[30]. One of the active compound apigenin from this plant has been recently studied for its synergistic effects of COVID-19 to HIV patients through an integrated Pharmaco-BioInformatics approaches [31].

Given the broad spectrum of medicinal properties associated with *I. tictoria*, this study endeavors to explore its potential antidiabetic property through molecular docking studies, pharmacophore modelling and ADMET profiling. The swift and cost-effectiveness determination of the antidiabetic mechanism of compounds isolated from medicinal plants is facilitated by in-silico virtual screening techniques. Various diabetes targets, including α-amylase, α-glucosidase, dipeptidyl peptidase-4 (DPP-4), glycogen synthase kinase-3β (GSK-3β), protein tyrosine phosphatase 1B (PTP1B), glucokinase, and peroxisome proliferator-activated receptors (PPARs) can be efficiently assessed through these methods [32]–[35].

Three subtypes namely α, δ, and γ, are recognized for peroxisome proliferator-activated receptors (PPARs). Among them, peroxisome proliferator-activated receptor- gamma (PPARγ) exists in two forms: PPARγ-1 and PPARγ-2. PPARγ-1 is predominantly expressed in the gut, whereas PPARγ-2 exhibits widespread expression in adipose tissue, playing a pivotal role in adipocyte differentiation and proliferation. The activation of the PPARγ receptor and the enhancement of insulin sensitivity are achieved by PPARγ agonists such as thiazolidinediones (TZD), function by stabilizing the ligand-binding domain (LBD)'s AF2 (activation function 2) in its active conformation [34], [36], [37].

This study aims to uncover the potential of phytochemicals found in *I. tinctoria* as PPARγ agonists, with the overarching goal of advancing the development of novel and enhanced antidiabetic agents. In this study, a computational approach was utilized to screen and asses phytoconstituents derived from *I. tinctoria*, evaluating their potential as PPARγ agonists for the treatment of diabetes mellitus.

2.0 Materials and methods:

2.1 Protein preparation:

The crystal structure of peroxisome proliferator-activated receptor gamma (PPARγ) (PDB ID: 3DZY) was retrieved from Protein Data Bank (PDB) repository [38] in pdb format. Protein was prepared with Autodock Tools- 1.5.7.[39]. Previously docked ligands with protein and water molecules were removed. Polar Hydrogens and Kollman charges were added to the protein and finally saved in PDBQT format.

2.2 Ligand preparation:

Twenty-one compounds from *I. tinctoria*, obtained by the IMPPAT website (Indian Medicinal Plants, Phytochemistry And Therapeutics) [40] were retrieved from PubChem Data Bank [41] in 3D .sdf format. The ligands and drug molecules Thiazolidinediones [Rosiglitazone (Avandia) and Pioglitazone (Actos)] were converted into pdb format using BIOVIA Discovery Studio Visualizer software[42]. The pdb format of ligand and drug molecules was converted into PDBQT format with Autodock Tools- 1.5.7.

2.3 Protein-ligand docking:

The docking calculations were performed using the AutoDock Vina version 1.1.2 software suite [43]. Flexible Blind docking was performed by applying a gridbox (center_x= 3.528, center_y= 29.000, center_z= 21.151 and size_x= 86, size_y=98, size_z=92) prepared to cover the whole protein with an exhaustiveness value of Ten. The contributions of intramolecular hydrogen bonds, hydrophobic, ionic, and Van der Waals interactions between docked protein and ligand complexes were used to determine the free energy (ΔG) specifying affinity scoring of the binding. After docking best pose (with zero lower and upper rmsd value) was chosen for further analysis. The docked protein-ligand complexes were created and the binding sites were analyzed to construct a 2D and 3D representation of the ligand interaction for each complex using BIOVIA Discovery Studio Visualizer software.

2.4 Computation of Inhibition Constant:

The molecular docking analysis predicts the inhibition constant (Ki value), which is used to evaluate the

Journal of Chemical Health Risks

www.jchr.org

JCHR (2023) 13(6), 2706-2720 | ISSN:2251-6727

effectiveness of the interaction. It also considers changes in hydrogen bonds formed with the protein's active site residues and predicted binding energies. The inhibition constant, or Ki value of the docked enzyme-inhibitor complex' is the Dissociation constant (Kd). Lower dissociation probability and hence higher inhibition are associated with smaller Ki values. The formula Ki =exp(ΔG/(RT) is used to calculate it, where T is the temperature (298.15 K), R is the gas constant (1.987 Kcal/K/mol), and ΔG is the free energy of binding[44].

2.5 Validation of molecular docking results:

Prior to molecular docking, we used the Castp online server to perform binding pocket analysis and predict the active site of protein 3DZY. CASTp (Computed Atlas of Protein Surface Topography) is a web-based tool for recognizing, characterizing, and measuring specific geometric and topological characteristics of protein structures [45]. Intact PPAR gamma - RXR alpha Nuclear Receptor Complex on DNA bound with Rosiglitazone in pocket Id 1 (Fig. 1) shows binding with residues of chain A ARG202, GLU203, VAL205 and GLN206 and with chain D ASN335, LYS336 and ASN 375 which matched with our redocking result with Rosiglitazone (Table 1).

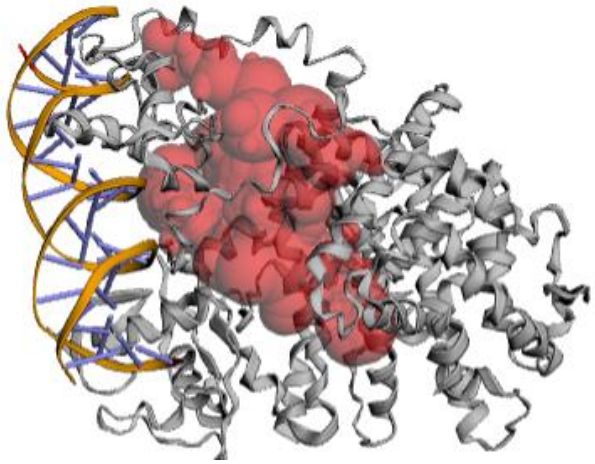

Fig. 1 Intact PPARγ - RXR alpha Nuclear Receptor Complex on DNA bound with Rosiglitazone, 9-cis Retinoic Acid and NCOA2 Peptide (PDB Id: 3DZY)

2.6 Screening of Ligands for Pharmacodynamics Properties:

The ligand molecules and drug molecules Thiazolidinediones [Rosiglitazone (Avandia) and Pioglitazone (Actos) Standard drugs for T2DM) were analyzed by Molinspiration [46] an online screening server. SMILES (Simplified Molecular Input Line Entry System) of these two molecules were used to generate a 3D structure and .mol file was used for the calculation of molecular properties and bioavailability scores. The larger the value of the bioactivity score is, the higher the probability that the particular molecule will be active.

2.7 Screening of Ligands for Pharmacokinetics and Drug-Likeness

Pharmacokinetics and Toxicity of candidate molecules decide them to be a drug molecule. In the early stages of Computer Added Drug Design (CADD), Absorption, Distribution, Metabolism, Excretion, and Toxicity (ADMET) of chemicals have been recognized as important considerations. The SwissADME [47], pkCSM [48] and ADMETLAB2.0 [49] web tools were used to evaluate the Pharmacokinetics, drug-likeness, and medicinal chemistry of these molecules. The SMILES format of the molecules were entered, and 2D structure files were generated in these tools. Several parameters were analyzed to check the ADMET properties of these molecules Important parameters for a drug molecule include pharmacokinetics parameters like P-glycoprotein, HIA (human intestinal absorption), drug-likeness prediction Lipinski, Ghose, and Veber criteria, and the BBB (Blood-Brain Barrier penetration). In order to evaluate drug-likeness and ascertain whether a compound is likely to be bioactive, a number of additional crucial parameters were employed, including molecular weight, LogP, number of HBA and HBD, as well as the Lipinski, Ghose, and Veber guidelines. Most "drug-like" compounds have logP ≤ 5, molecular weight (MW) ≤ 500, number of hydrogen bond acceptors (nHA) ≤ 10, and number of hydrogen bond donors (nHD) ≤ 5, according to Lipinski's "Rule of 5" [50]. If a molecule violates multiple principles, it might face issues with its bioavailability. The human intestinal absorption, bioavailability, Caco-2 (human epithelial colorectal adenocarcinoma cell line), monolayer permeability, and blood-brain barrier penetration can all be described by the ideal descriptor, LogP (octanol/water partition coefficient), Topological Polar Surface Area (TPSA). These factors play a significant role in predicting the qualities of drug.

3.0 Results and Discussion:

3.1 Molecular docking and Molecular interactions (2D and 3D) analysis

Molecular docking and virtual screening, rational drug design (RDD) or computer-aided drug design (CADD), offering a swift cost-effective and dependable approach to discovering novel drugs (lead molecules) and potential druggable protein targets. In this study, we employed molecular docking-based virtual screening to pinpoint a promising target for Type 2 diabetes Millitus (T2DM). Following a comprehensive literature review and considering available crystal structures of proteins pivotal in T2DM's biosynthetic pathways [51], [52], we have selected peroxisome proliferator-activated receptor gamma (PPARγ) (PDB ID: 3DZY). This in-silico

Journal of Chemical Health Risks

www.jchr.org

JCHR (2023) 13(6), 2706-2720 | ISSN:2251-6727

investigation delved into the likely molecular docking interactions between the selected 21 phytochemicals and the PPARγ. The findings were juxtaposed with established T2DM drugs Rosiglitazone (Avandia) and Pioglitazone (Actos). Out of the 21 compounds, 18 exhibited superior binding energies of -9.4 kcal/mol, -9.1 Kcal/mol, -9.0 Kcal/mol, -8.9 Kcal/mol, -8.8 Kcal/mol, -8.7 Kcal/mol, -8.6 Kcal/mol, -8.4 Kcal/mol, -8.3 Kcal/mol, -8.2 Kcal/mol, -8.0 Kcal/mol, -7.9 Kcal/mol, -7.4 Kcal/mol and -6.9 Kcal/mol compared to the binding energies of two drug molecules Rosiglitazone (-6.5 Kcal/mol) and Pioglitazone (-6.9 Kcal/mol) (Table 1). The binding affinity (Kcal/mol) of the ligand or inhibitor serves as a metric to correlate and scrutinize with the corresponding protein target. Generally, a lower binding energy indicates a higher affinity (more negative) of the ligand for the receptor protein. Consequently, the ligand demonstrating the utmost affinity emerges as a promising candidate warranting further research.

Table 1. Auto Dock Vina docking results showing binding affinities and inhibition constant of Ligands and Drug Molecules with $PPAR_{\Upsilon}$ protein (PDB Id: 3DZY) related to diabetes mellitus.

S. No.	Ligand name	PubChem CID	Binding Affinity (ΔG) (kcal/mol)	Inhibition Const. Ki (μM)	No. of H-Bonds	H-Bond Forming Residues	H-Bond length (A^0)	*Other Types of bonds within Ligand-Protein Complex (No. of Other bonds)
1	Pseudosemiglabrin	156341	-9.4	0.13	2	D:THR349 A:ASP176	2.19623 3.50314	Pi-Sulfur, Pi-Alkyl (3)
2	Dehydrodeguelin	3083803	-9.1	0.21	1	A:CYS190	3.27964	Pi-Cation, Pi-Pi T –shaped, Alkyl, Pi-Alkyl (5)
3	Apigenin	5280443	-9.0	0.25	2	A:ALA327 A:ASN306	1.94102 2.32653	Pi-Alkyl (5)
4	Tephrosin	114909	-8.9	0.30	2	D:SER355 D:SER355	2.02596 2.17744	Alkyl Pi-Alkyl (3)
5	Indirubin	10177	-8.9	0.30	2	A:GLN193 A:LYS175	2.68838 2.48328	Pi-Alkyl Unfav. Donor-Donor (4)
6	Indigo	10215	-8.8	0.35	1	A:LYS175	1.85685	Pi-Pi T –shaped, Pi-Alkyl (4)
7	Comp. 7*	182678	-8.7	0.42	---	---	---	Pi-Sulfur, Pi-Alkyl (2)
8	Luteolin	5280445	-8.6	0.49	3	D:SER355 A:CYS190 D:TYR250	2.08969 2.26087 2.65263	Pi-Alkyl (2)
9	Deguelin	107935	-8.6	0.49	1	D:SER355	2.16122	Alkyl, Pi-Alkyl (3)
10	Quercetin	5280343	-8.6	0.49	3	A:ASP176 A:CYS177	2.17165 2.14544	Pi-Alkyl (2)

Journal of Chemical Health Risks

www.jchr.org

JCHR (2023) 13(6), 2706-2720 | ISSN:2251-6727

						D:SER355	2.31569	
11	Rotenone	6758	-8.4	0.69	2	D:TYR250 A:ASP176	1.96156 3.41319	Pi-Anion, Alkyl (2)
12	Sumatrol	442824	-8.3	0.82	1	D:SER355	1.89955	Alkyl, Pi-Alkyl (4)
13	Rotenol	44257420	-8.2	0.97	2	D:SER355 A:GLN193	2.30255 3.31966	Pi-Pi- Stacked, Alkyl, Pi-Alkyl (5)
14	Kaempferol	5280863	-8.0	1.36	---	---	---	Pi-Alkyl (2)
15	Galactomannan	439336	-7.9	1.61	5	A:CYS177 A:CYS190 D:TYR250 A:ASP176 A:GLN193	2.55694 2.73152.97745 3.01804 3.20024	---
16	Indican	441564	-7.4	3.76	5	A:CYS190 D:TYR250 A:LYS175 D:TYR250 A:GLN193	2.32489 2.11049 2.53092 3.38986 3.37266	Pi-Alkyl (3)
17	Coumarin	323	-6.9	8.74	---	---	---	Pi-Sig., Pi-Pi- Stacked, Amide Pi- Stacked, Pi-Alkyl (11)
18	Indicine	73614	-6.9	8.74	2	A:LEU309 A:ILE268	2.78231 3.50636	---
19	1H-Indol-3-ol	50591	-5.9	47.29	2	D:THR349 A:TYR189	2.11718 2.53938	Pi-Alkyl (1)
20	D-Galactose	6036	-5.6	78.48	4	A:TYR169 A:GLN193 A:TYR169 D:ASO337	2.01964 2.45222 2.39029 2.19292	---
21	D-Mannose	18950	-5.6	78.48	2	A:TYR169	2.20191	---

Journal of Chemical Health Risks

www.jchr.org

JCHR (2023) 13(6), 2706-2720 | ISSN:2251-6727

						A:LEU167	2.69919	
22	Pioglitazone	4829	-6.9	8.74	2	A:ILE179	2.49221	---
						D:TYR250	2.50474	
23	Rosiglitazone	77999	-6.5	17.18	5	D:LYS336	2.52141.99595	Pi-Anion Pi-Alkyl (2)
						D:ASN375	2.00842	
						A:VAN205	3.40321	
						D:ASN335	3.52056	
						A:GLN206		

*[(12S,15R,16R)-14,14-dimethyl-6-oxo-4-phenyl-3,11,13-trioxatetracyclo[8.6.0.02,7.012,16]hexadeca-1(10),2(7),4,8-tetraen-15-yl] acetate

About Twenty one compounds derived from *I. tinctoria* (Table 1), screened against 3DZY, in which six (6) top posed compounds exhibited the highest binding affinities against the protein target and were selected for post docking analysis. From the multiple screening analysis, the following compounds Pseudosemiglabrin (PubChem CID: 156341), Dehydrodeguelin (PubChem CID: 3083803), Apigenin (PubChem CID: 5280443), Tephrosin (PubChem CID: 114909), Indirubin (PubChem CID:10177) Indigo (PubChem CID: 10215) showed the lowest docking scores (highest binding affinity scores) against PDB 3DZY. This virtual screening based on binding energy gave us a vivid idea of the best ligands having the highest affinity for the receptor protein. Human adipogenesis, insulin sensitivity, and glucose homeostasis are all regulated by PPARγ, a significant transcriptional factor [53], [54], for which the drug rosiglitazone, is an excellent sensitizer to insulin and enhances glucose absorption and reduces hyperglycemia and hyperinsulinemia [55]–[57]. The ineffectiveness of PPAR-gamma receptors to stimulate transcription was demonstrated by their reduced capacity to bind DNA in response to rosiglitazone and also potential therapeutic targets to treat inflammation, atherosclerosis, and hypertension. A comprehensive literature survey showed that in the crystal structures of PPAR-gamma and rosiglitazone complex, binding pockets of the intact PPAR-gamma receptor interact with the rosiglitazone, especially with The GLN193, TYR189, LEU196, ALA197, TYR192, GLU203, LYS201, ARG202, LYS336, ASN335, ASP337, LEU237, PHE347, VAL248, GLU351, and TYR250 residues [57]. In our investigation rosiglitazone binds with PDB 3DZY with three conventional hydrogen bonds with residues D:LYS336, D:ASN375, A:VAN205, having bond lengths 2.5214 A^0, 1.99595 A^0 and 2.00842 A^0 and two Carbon Hydrogen bonds with residues D:ASN335 and A:GLN206 having bond lengths 3.40321 A^0 and 3.52056 A^0 . Two more bonds with A:GLU203 (Pi – Anion of bond length 4.25844 A^0) and with A:ARG202 (Pi – Alkyl of bond length 5.33718 A^0) are also found which validates molecular docking protocol.

Compound Pseudosemiglabrin (PubChem CID: 156341), having highest binding affinity (-9.4 kcal/mol), forms two Hydrogen bonds with residues D:THR349 (2.19623 A^0) and A:ASP176 (3.50314 A^0). Besides these it also showed 3 more bonds (one Pi-Sulfur with A:CYS190 of bond length 5.9546 A^0 and two Pi- Alkyl bonds with A:LYS175 and A:LYS194 of bond lengths 4.75983 A^0 and 4.85541 A^0), which stabilizes the complex and provides highest binding affinity to the complex (Table 1, Fig 1a and 1b). Dehydrodeguelin (PubChem CID: 3083803) having binding affinity (-9.1 K cal/mol) formed one Hydrogen bond (3.27964 A^0) with residue A:CYS190 and five other (one Pi-Cation with A:LYS194, one Pi-Pi T – shaped with D:TYR250, two Alkyl bond with A:LEU178 and one Pi-Alkyl bond with A:LYS194) of bond lengths respectively 4.57386 A^0, 5.34733 A^0, 5.41055 A^0, 5.2767 $A^0$and 5.32275 A^0. Apigenin (PubChem CID: 5280443), having bindin affinity (-9.0 K cal/mol), also binds efficiently with two hydrogen bonds with A:ALA327 (1.94102 A^0) and A:ASN306 (2.3265 A^0) and Five Alkyl bonds with residues ILE310, CYS432, LEU436, ALA271 and LEU309 of chain A (bond lengths around 4-5 A^0)

Compounds Tephrosin (PubChem CID: 114909), Indirubin (PubChem CID:10177) and Indigo (PubChem CID: 10215) showed binding affinity of -8.9 Kcal/mol to -8.8 Kcal/mol. Tephrosin having two Hydrogen bonds with D:SER355 (2.02596 A^0 and 2.17744 A^0) including three other types of bonds (Alkyl and Pi-Alkyl) with A:LYS175 of bond length around 4.77 A^0.

Journal of Chemical Health Risks

www.jchr.org

JCHR (2023) 13(6), 2706-2720 | ISSN:2251-6727

Indirubin also exhibits two hydrogen bonds with A:GLN193 and A:LYS175 (2.68838 A^0 and 2.48328 A^0) and four other types of bonds with residues A:LYS175, A:CYS190, A:LYS194 and one unfavourable dodor-donor bond. Indigo also showed one strong Hydrogen bond with A:LYS175 (of shortest bond length 1.85685 A^0) and four other types of bonds with A: TYR189, A:LYS194, A:LYS175 (bond lengths between 5.2346 A^0 to 5.98541 A^0). Other compounds[(12S,15R,16R)-14,14-dimethyl-6-oxo-4-phenyl-3,11,13-trioxatetracyclo[8.6.0.02,7.012,16]hexadeca-1(10),2(7),4,8-tetraen-15-yl] acetate, Luteolin, Deguelin, Quercetin, Rotenone, Sumatrol, Rotenol, Kaempferol, Galactomannan, Indican and Coumarin also showed better biding affinities to 3DZY in comparison to well known drugs Pioglitazone and Rosiglitazone (-6.9 Kcal/mol and -6.5 k cal/mol) for T2DM mellitus. These whole findings are summarized in Table 1. Fig. 2a- 24b depicts the 3D and 2D diagrams of different phytochemicals showing H –bond donor and receptor regions with bindings of residues in active sites of the protein 3DZY.

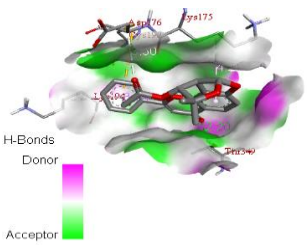

Fig. 2a

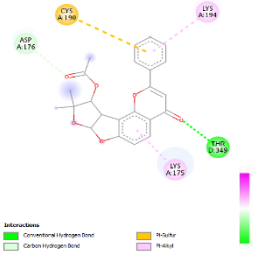
Fig. 2b

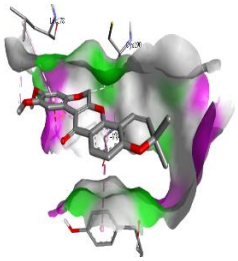
Fig. 3a

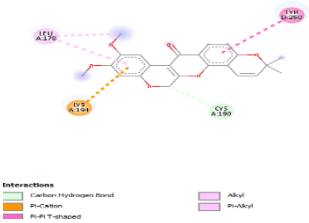
Fig. 3b

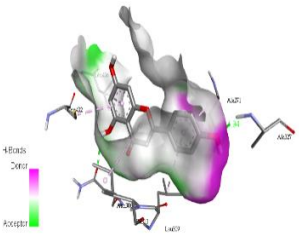
Fig. 4a

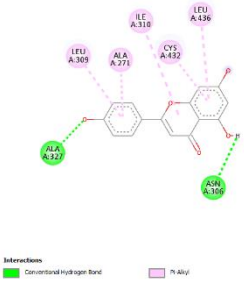
Fig. 4b

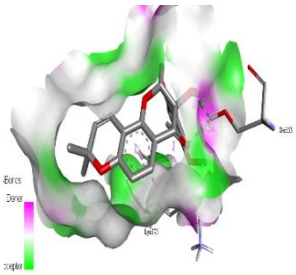
Fig. 5a

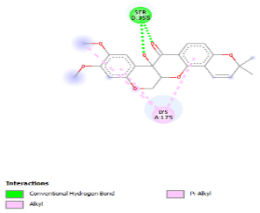
Fig. 5b

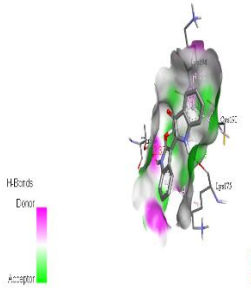
Fig. 6a

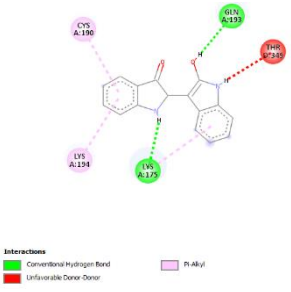
Fig. 6b

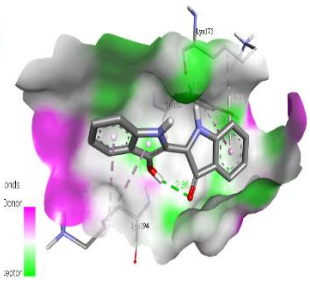
Fig. 7a

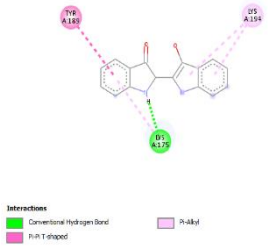
Fig. 7b

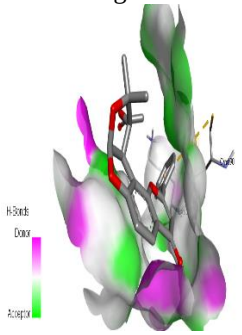
Fig. 8a

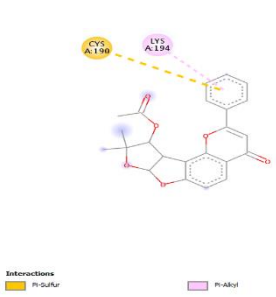
Fig. 8b

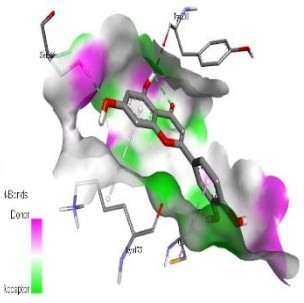
Fig. 9a

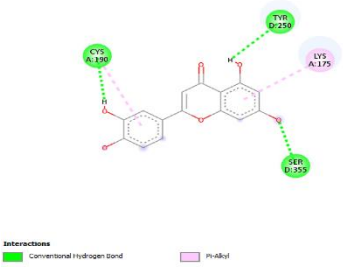
Fig. 9b

Journal of Chemical Health Risks

www.jchr.org

JCHR (2023) 13(6), 2706-2720 | ISSN:2251-6727

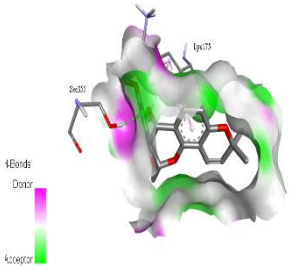

Fig. 10a

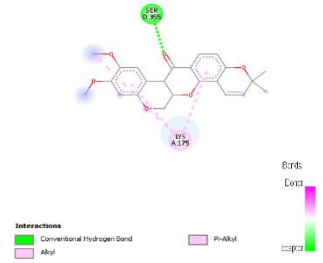

Fig. 10b

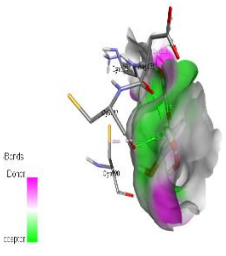

Fig. 11a

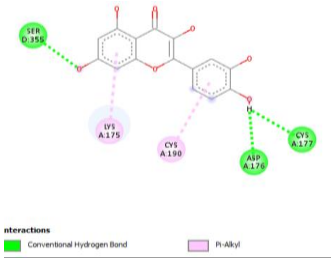

Fig. 11b

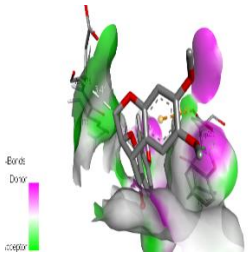

Fig. 12a

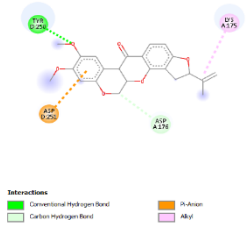

Fig. 12b

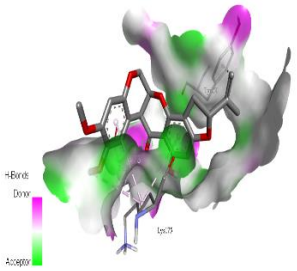

Fig. 13a

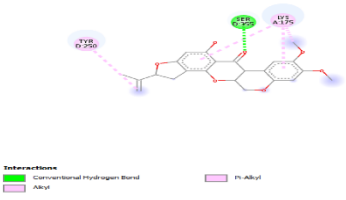

Fig. 13b

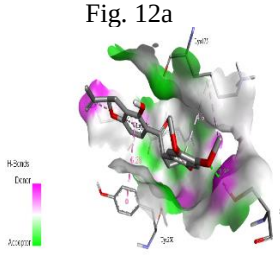

Fig. 14a

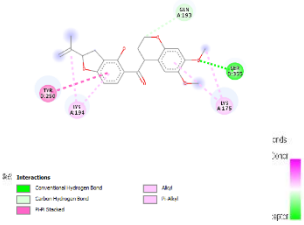

Fig. 14b

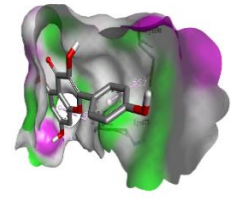

Fig. 15a

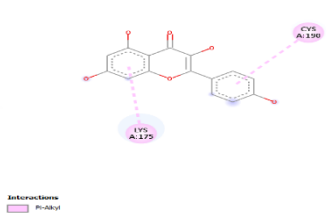

Fig. 15b

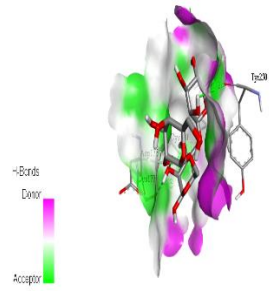

Fig. 16a

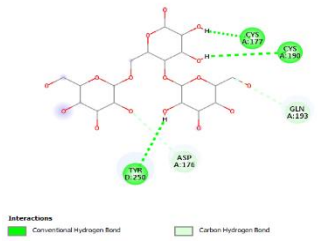

Fig. 16b

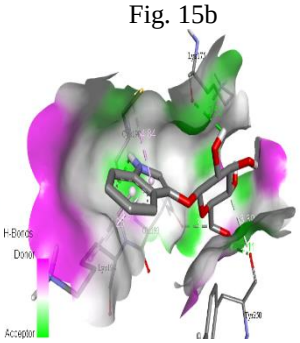

Fig. 17a

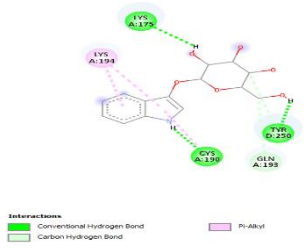

Fig. 17b

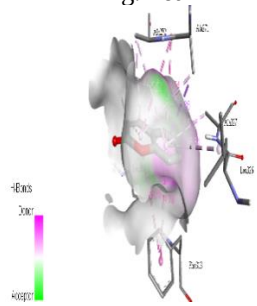

Fig. 18a

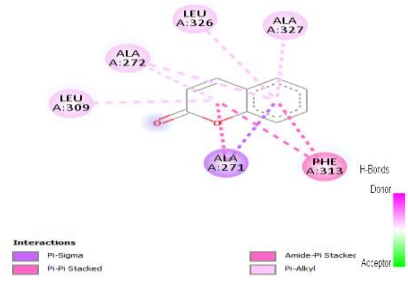

Fig. 18b

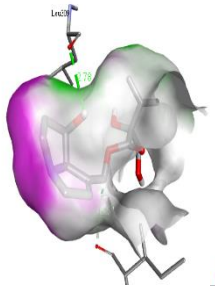

Fig. 19a

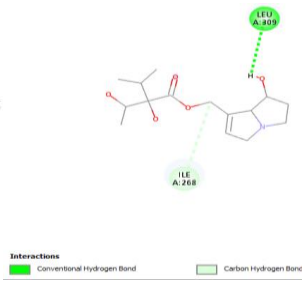

Fig. 19b

Journal of Chemical Health Risks

www.jchr.org

JCHR (2023) 13(6), 2706-2720 | ISSN:2251-6727

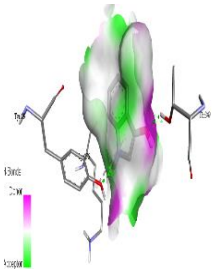

Fig. 20a

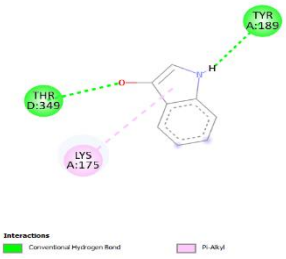

Fig. 20b

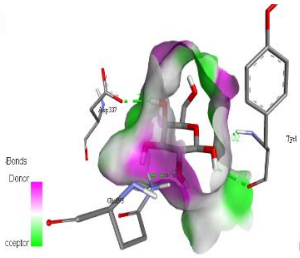

Fig. 21a

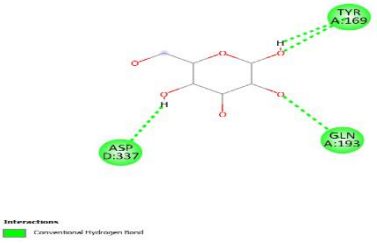

Fig. 21b

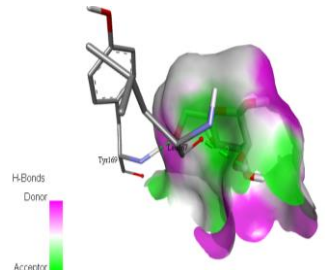

Fig. 22a

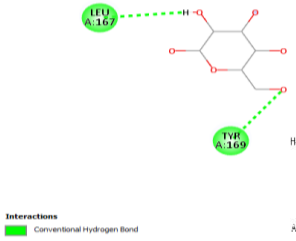

Fig. 22b

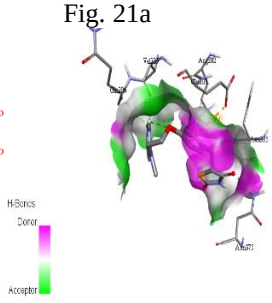

Fig. 23a

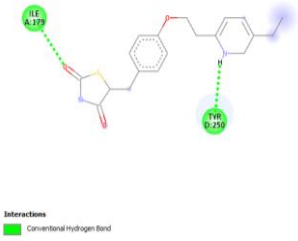

Fig. 23b

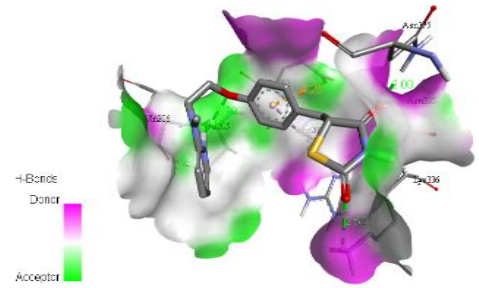

Fig. 24a

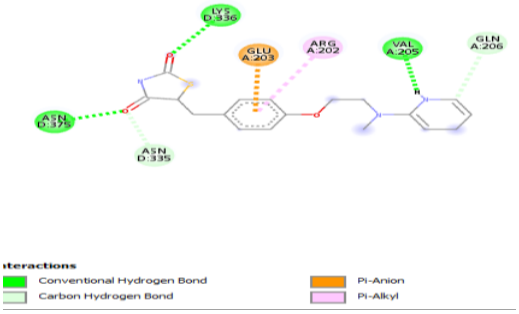

Fig. 24b

Fig 2-24. All twenty one phytochemicals and two drug molecules (in Table1, S. No. 1-23) docked with human peroxisome proliferator-activated receptor-gamma [PPAR-gamma (PDB ID: 3DZY)]. (a) The 3D image shows significant interactions with donor and accepter H –bonds regions (b) The molecular level interactions of binding-pocket residues with the molecules are depicted in the 2D plot.

3.2 Pharmacodynamics of Ligands and Drug Molecules:

The molinspiration bioactivity score (v22.08 beta) and Molecular properties have been calculated for ligands and drug molecules are presented (in Table 2) for active drug-likeness towards parameters like ion channel modulators, kinase inhibitors, GPCR ligands, nuclear receptor ligands, protease inhibitors, and other enzyme inhibitors. On comparison it is seen that bioactivity score for each parameter of top posed six compounds Indirubin and Indigo showed much better kinase inhibition (0.93, 0.76) in comparison to both drug molecules (-0.71, -0.61), nuclear receptor score is average. But enzyme inhibition score for all compounds (except dehydrodeguelin) is much higher than the drug molecules.

Table 2. Predicted Bioactivity score of ligands and drug molecules**:**

S.No	Parameter	Pseudosemiglabrin	Dehydrodeguelin	Apigenin	Tephrosin	Indirubin	Indigo	Pioglitazone	Rosiglitazone
1	GPCR ligand	0.10	-0.19	-0.07	0.08	0.11	0.28	0.25	0.15
2	Ion channel modulator	-0.19	-0.58	-0.09	-0.22	0.10	-0.01	-0.51	-0.65

Journal of Chemical Health Risks

www.jchr.org

JCHR (2023) 13(6), 2706-2720 | ISSN:2251-6727

3	Kinase inhibitor	0.00	-0.20	0.18	-0.22	0.93	0.76	-0.71	-0.61
4	Nuclear receptor	0.23	0.34	0.34	0.28	0.19	0.24	0.64	0.35
5	Protease inhibitor	-0.04	-0.39	-0.25	-0.05	-0.20	0.02	-0.09	-0.21
6	Enzyme inhibitor	0.46	0.01	0.26	0.37	0.21	0.35	0.05	-0.07

3.3 Pharmacokinetics and ADMET Evaluation of ligands and drug molecules:

The pharmacokinetic and drug-likeness data are presented in Table 3 and Table 4. According to the pharmacokinetic/ADMET properties, ligands and drug molecules both showed high human intestinal absorption (HIA). Compound 1-3 showed lower (0.0-0.1), compound 4 (0.1-0.3), compound 5 and compound 6 (0.3-0.5) slightly higher BBB permeability. Fig. 2a depicts their HIA and BBB permeability (white and boiled egg portion). The human colon epithelial cancer cell line, Caco-2, is used as a model of human intestinal absorption of drugs. Caco-2 Permeability of all molecules was found to be nearly same as both the drug molecules. Drug-likeness prediction was also performed for Lipinski Rule, Pfizer Rule, GSK Rule and Golden Triangle rule. All compounds were found to accept Lipinski rule of 5 and Golden Triangle rule, but Pfizer rule and GSK rules were rejected by some compounds (these rules are not of more concerns). Compound Apigenin, which accepted all rules as drug molecule Pioglitazone. Meanwhile, all compounds have physicochemical, molecular, and ADMET properties between the upper and lower predicted values (Table 2, 3, 4 and Fig. 25a, 25b). QED value (a measure of drug likeness based on the concept of desirability) for Tephrosin (0.814) was found to be much higher than both the drug molecules, while for other molecules is greater than 0.5, indicating favorable drug likeness for these molecules. AMES toxicity finding (Table 4) indicate that compound 1 has slightly toxic (>0.5), whereas compound 2-6 are less toxic. Thus on the basis of the above findings it may be concluded that most of the bioactive compounds (especially top six posed) from *I. tinctoria* may act as more active inhibitors for PPAR$_\gamma$ insulin receptor protein as Pioglitazone and Rosiglitazone drug molecules.

Table 3. Predicted Physico-chemical, Druglikeness and Molecular properties of ligands and drug molecules:

S/N	Parameter	Comp. 1	Comp. 2	Comp. 3	Comp. 4	Comp. 5	Comp. 6	Drug. 1	Drug. 2
1	miLogP	4.22	4.42	2.26	3.01	3.11	2.86	3.07	2.35
2	TPSA	74.98	67.15	90.89	83.47	65.98	65.98	68.30	71.53
3	natoms	29	29	20	30	20	20	25	25
4	MW	392.41	392.41	270.24	410.42	262.27	262.27	356.45	357.44
5	nON (HBA*)	6	6	5	7	4	4	5	6
6	nOHNH (HBD**)	0	0	3	1	2	2	1	1
7	Lipinski Ro5	Accepted	Accepted	Accepted	Accepted	Accepted	Accepted	Accepted	Accepted
	Pfizer	Rejected	Rejected	Accepted	Accepted	Rejected	Rejected	Rejected	Accepted
	GSK	Rejected	Accepted	Accepted	Rejected	Accepted	Accepted	Accepted	Accepted
	Golden Triangle	Accepted	Accepted	Accepted	Accepted	Accepted	Accepted	Accepted	Accepted
8	nrotb	3	2	1	2	1	1	7	7
9	volume	340.92	341.42	224.05	2355.15	223.85	223.85	318.53	314.51

Note: *HBA: Hydrogen Bond Acceptors (as total number of nitrogen and oxygen atoms),
**HBD: Hydrogen Bond Donors (as total number of oxygen−hydrogen and nitrogen−hydrogen bonds)

Table 4. In silico Pharmacokinetics, ADMET properties and Drug-likeness of studied Molecules:

	Absorption		Distribution		Metabolism		Excretion and Toxicity	
S/N	Parameter	Predicted value (Comp. 1-6)	Parameter	Predicted value (Comp. 1-6)	Parameter	Predicted value (Comp. 1-6)	Parameter	Predicted value (Comp. 1-6)

Journal of Chemical Health Risks

www.jchr.org

JCHR (2023) 13(6), 2706-2720 | ISSN:2251-6727

1	Water Solubility (Log S)	-4.504 -5.227 -3.606 -4.623 -4.653 -4.271	Volume distribution (VD) of a drug in blood plasmas	1.580 0.629 0.510 0.945 0.367 0.384	CYP2 D6 inhibitor	- --- ++ -- - -	Total drug clearance log (CLtot)	1.647 2.561 7.022(high) 3.703 0.795 0.625
2	Lipid Solubility (Log P)	4.185 3.966 3.307 3.939 3.030 3.091			CYP3 A4 inhibitor	-- + ++ ++ + -	AMES toxicity, hERG I & II inhibitor	+ - -- - - +
3	Caco-2 Permeability	-4.725 -4.869 -4.847 -4.819 -4.947 -5.093	Plasma protein binding (PPB)	89.034% 89.694% 97.255% 93.534% 98.738% 99.499%	CYP1 A2 inhibitor	-- - +++ -- + +++		
4	Log Kp skin permeability	-6.32 cm/s -6.14 -5.80 -6.69 -5.96 -5.96	BBB permeability	--- --- --- -- - -	CYP2 C19 inhibitor	++ + ++ - - +		
5	Human intestinal absorption (HIA)	High High High High High High	The fraction unbound in blood plasmas (Fu)	8.085% 8.183% 3.668% 8.257% 1.161% 1.161%	CYP2 C9 inhibitor	--- + + + + +		
6	QED value (a measure of drug likeness) Attractive>0.67	0.614 0.637 0.632 0.814 0.707 0.707						

Note: For the classification endpoints, the prediction probability values are transformed into six symbols: 0-0.1(---), 0.1-0.3(--), 0.3-0.5(-), 0.5-0.7(+), 0.7-0.9(++), and 0.9-1.0(+++).

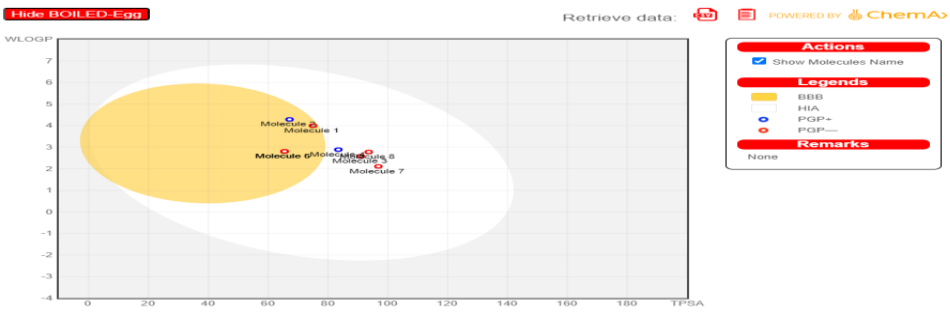

Fig.25a

Journal of Chemical Health Risks

www.jchr.org

JCHR (2023) 13(6), 2706-2720 | ISSN:2251-6727

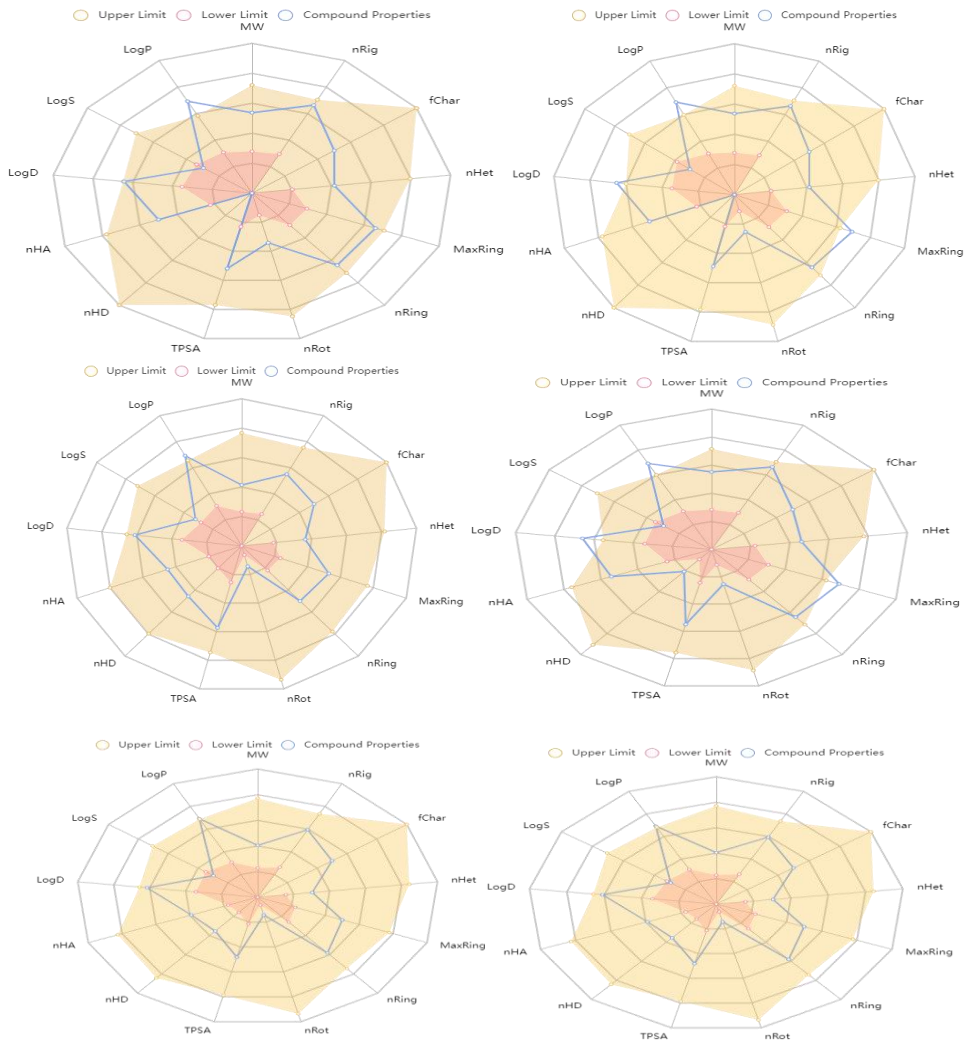

Fig. 25b

Fig. 25(a). BOILED-Egg plot of top six posed phytochemical compounds showing blood-brain barrier (BBB) penetration and human intestinal absorption (HIA) of ligands and drug molecules. Here PGP- shows the P-glycoprotein substrate negative nature while PGP+ shows the P-glycoprotein substrate positive nature.

25(b) Bioavailability radar of top six posed phytochemical compounds from *I. tinctoria*, based on physicochemical indices ideal for oral bioavailability. The pink zone in the bioavailability radar is the ideal physicochemical space for oral bioavailability. LIPO (lipophilicity: −0.7 < XLOGP3 < p 5); SIZE (molecular weight: 150 g/mol < mol wt < 500 g/mol); POLAR (polarity: 20 Å2 < TPSA < 140 Å2); INSOLU [insolubility: 0 < Log S (ESOL) < 6]; INSATU (insaturation: 0.25 < fraction C sp3 < 1); and FLEX (flexibility: 0 < number of rotatable bonds < 9).

Conclusions:

The global threat posed by diabetes mellitus and the adverse effects associated with current diabetes medications, the exploration of phytoconstituents with low toxicity emerges as a promising avenue. This study delved into the screening of 21 phytochemicals derived from the *I.tinctoria* plant, specifically targeting peroxisome proliferator-activated receptors (PPARs), notably PPAR$_\Upsilon$. These receptors play a pivotal role in regulating adipogenesis, insulin sensitization, and glucose homeostasis in humans. Molecular docking analyses uncovered six phytochemicals—Pseudosemiglabrin, Dehydrodeguelin, Apigenin, Tephrosin, Indirubin, and Indigo—that exhibited superior binding affinity with the target protein (PDB Id: 3DZY) compared to conventional PPAR$_\Upsilon$ agonists, such as Rosiglitazone and Pioglitazone. Notably, pharmacophore and ADMET studies provided evidence of their drug-like behavior without inducing acute toxicity. Additionally, other phytochemicals like Quercetin, Kaempferol, and Coumarin, previously studied for various medicinal properties, also demonstrated significant binding affinities for the PPAR$_\Upsilon$ receptor. In light of these findings, it is plausible

Journal of Chemical Health Risks

www.jchr.org

JCHR (2023) 13(6), 2706-2720 | ISSN:2251-6727

to anticipate that phytochemicals derived from *I. tinctoria* could emerge as promising candidates for developing a more effective and safer antidiabetic drug. The next crucial step involves subjecting these phytoconstituents to rigorous clinical trials to validate their potential therapeutic benefits and pave the way for their integration into mainstream diabetes treatment protocols. The future holds promise for harnessing the potency of these natural compounds in addressing the global health challenge posed by diabetes mellitus.

References:

[1] S. D. Gwatidzo en J. Stewart Williams, "Diabetes mellitus medication use and catastrophic healthcare expenditure among adults aged 50+ years in China and India: results from the WHO study on global AGEing and adult health (SAGE)", *BMC Geriatrics*, vol 17, no 1, bll 1–15, 2017, doi: 10.1186/s12877-016-0408-x.

[2] "International Diabetes Federation, Diabetes Atlas, 9th ed, Brussels, Belgium, 2019", 2019.

[3] V. P. Gaonkar en K. Hullatti, "Indian Traditional medicinal plants as a source of potent Anti-diabetic agents: A Review", *Journal of Diabetes and Metabolic Disorders*, vol 19, no 2, bll 1895–1908, 2020, doi: 10.1007/s40200-020-00628-8.

[4] "World Health Organization, 'The top 10 causes of deaths:,' Fact sheet 2020, 2020. https://www.who. int/news-room/fact-sheets/detail/the-top-10-causes-of-death", 2020.

[5] S. G. Jeyam M., Priyadharsini K., Ravikumar P., "Evaluating multi-target efficiency of phyto-compounds against diabetes mellitus—an in silico approach", *BIOINFO Drug Targets*, vol 2, no 1, bll 24–28, 2014.

[6] B. Lorenzati, C. Zucco, S. Miglietta, F. Lamberti, en G. Bruno, "Oral hypoglycemic drugs: Pathophysiological basis of their mechanism of action", *Pharmaceuticals*, vol 3, no 9, bll 3005–3020, 2010, doi: 10.3390/ph3093005.

[7] "American Diabetes Association, 'Strategies for Improving Care,' Diabetes Care, vol. 39, no. Sppule- ment 1, p. S6, 2016, doi: 10.2337/dc16-S004".

[8] Mooventhan A. and Nivethitha L., "A Narrative Review on Evidence-based Antidiabetic Effect of Fenu- greek (Trigonella Foenum-Graecum), https://doi.org/10.4103/ijnpnd.ijnpnd", *Int J Nutr Pharmacol Neurol Dis.*, vol 7, bll 84–87, 2017.

[9] S. Vincent, S. Arokiyaraj, M. Saravanan, en M. Dhanraj, "Molecular Docking Studies on the Anti-viral Effects of Compounds From Kabasura Kudineer on SARS-CoV-2 3CLpro", *Frontiers in Molecular Biosciences*, vol 7, no December, bll 1–12, 2020, doi: 10.3389/fmolb.2020.613401.

[10] R. R. Narkhede, R. S. Cheke, J. P. Ambhore, en S. D. Shinde, "The Molecular Docking Study of Potential Drug Candidates Showing Anti-COVID-19 Activity by Exploring of Therapeutic Targets of SARS-CoV-2", *Eurasian Journal of Medicine and Oncology*, vol 4, no 3, bll 185–195, 2020, doi: 10.14744/ejmo.2020.31503.

[11] T. E. Tallei *et al.*, "Potential of Plant Bioactive Compounds as SARS-CoV-2 Main Protease (Mpro) and Spike (S) Glycoprotein Inhibitors: A Molecular Docking Study", *Scientifica*, vol 2020, 2020, doi: 10.1155/2020/6307457.

[12] P. Bansal, R. Kumar, J. Singh, en S. Dhanda, "In silico molecular docking of SARS-CoV-2 surface proteins with microbial non-ribosomal peptides: identification of potential drugs", *Journal of Proteins and Proteomics*, vol 12, no 3, bll 177–184, 2021, doi: 10.1007/s42485-021-00072-z.

[13] H. I. Umar, B. Siraj, A. Ajayi, T. O. Jimoh, en P. O. Chukwuemeka, "Molecular docking studies of some selected gallic acid derivatives against five non-structural proteins of novel coronavirus", *Journal of Genetic Engineering and Biotechnology*, vol 19, no 1, 2021, doi: 10.1186/s43141-021-00120-7.

[14] R. Suravajhala *et al.*, "Molecular docking and dynamics studies of curcumin with COVID-19 proteins", *Network Modeling Analysis in Health Informatics and Bioinformatics*, vol 10, no 1, bll 1–10, 2021, doi: 10.1007/s13721-021-00312-8.

[15] S. WANARASE, S. CHAVAN, en S. SHARMA, "a Molecular Docking Study: Targeting Covid-19 (Sars-Cov-2) Main Protease Using Active Phytocompounds From Terminalia Arjuna", *Innovare Journal of Medical Sciences*, vol 10, no 5, bll 9–14, 2022, doi: 10.22159/ijms.2022.v10i5.46122.

[16] K. Karthick en K. Swarnalatha, "Pyridine Derivatives as Potential Inhibitors for Coronavirus SARS-CoV-2: A Molecular Docking Study", *Bioinformatics and Biology Insights*, vol 17, 2023, doi: 10.1177/11779322221146651.

[17] M. B. Azmi *et al.*, "In Silico Characterization of Withania coagulans Bioactive Compounds as Potential Inhibitors of Hydroxymethylglutaryl (HMG-CoA) Reductase of Mus musculus", *ACS Omega*, vol 8, no 5, bll 5057–5071, 2023, doi: 10.1021/acsomega.2c07893.

Journal of Chemical Health Risks

www.jchr.org

JCHR (2023) 13(6), 2706-2720 | ISSN:2251-6727

[18] M. A. H. Mostafa, H. M. J. Khojah, en T. Ohta, "Isolation and identification of novel selective antitumor constituents, sidrin and sidroside, from Zizyphus spina-christi", *Saudi Pharmaceutical Journal*, vol 31, no 6, bll 1019–1028, 2023, doi: 10.1016/j.jsps.2023.04.029.

[19] W. K. Campbell-Tofte J. I., Mϕlgaard P., "Harnessing the potential clinical use of medicinal plants as antidiabetic agents", *Bot. Targets Ther.*, vol vol.2, no 10, bll 7–19, 2012.

[20] M. Yaqub Khan, I. Aziz, B. Bihari, H. Kumar, M. Roy, en V. Kumar Verma, "a Review-Phytomedicines Used in Treatment of Diabetes", *International Journal of Pharmacognosy*, vol 1, no 6, bll 343–65, 2014, [Online]. Available at: http://dx.doi.org/10.13040/IJPSR.0975-8232.IJP.1

[21] A. N. Sadasivan Nair *et al.*, "Antidiabetes constituents, cycloartenol and 24-methylenecycloartanol, from ficus krishnae", *PLoS ONE*, vol 15, no 6, bll 1–21, 2020, doi: 10.1371/journal.pone.0235221.

[22] P. K. Singh, J. Singh, T. Medhi, en A. Kumar, "Phytochemical Screening, Quantification, FT-IR Analysis, and in Silico Characterization of Potential Bio-active Compounds Identified in HR-LC/MS Analysis of the Polyherbal Formulation from Northeast India", *ACS Omega*, vol 7, no 37, bll 33067–33078, 2022, doi: 10.1021/acsomega.2c03117.

[23] Anshika *et al.*, "Plant bioactive compounds and their mechanistic approaches in the treatment of diabetes: a review", *Future Journal of Pharmaceutical Sciences*, vol 8, no 1, 2022, doi: 10.1186/s43094-022-00443-3.

[24] D. D. Joshi, L. Deb, B. G. Somkuwar, en V. S. Rana, "Relevance of Indian traditional tisanes in the management of type 2 diabetes mellitus: A review", *Saudi Pharmaceutical Journal*, vol 31, no 5, bll 626–638, 2023, doi: 10.1016/j.jsps.2023.03.003.

[25] O. S. Okoh *et al.*, "Identification of some bioactive compounds from Trignonella foenumgraecumas possible inhibitors of PPARU for diabetes treatment through molecular docking studies, pharmacophore modelling and ADMET profiling: An in-silico study", *PLoS ONE*, vol 18, no 5 May, bll 1–15, 2023, doi: 10.1371/journal.pone.0284210.

[26] A. Singh, *Medicinal Plants of the World*. 2006.

[27] T. R. Kameswaran en R. Ramanibai, "The antiproliferative activity of flavanoidal fraction of Indigofera tinctoria is through cell cycle arrest and apoptotic pathway in A-549 cells", *Journal of Biological Sciences*, vol 8, no 3, bll 584–590, 2008, doi: 10.3923/jbs.2008.584.590.

[28] B. & M. A. Bai, R & Madakkannu, "Preliminary phytochemical screening and in vitro antioxidant activities of aqueous extract of Indigofera tinctoria and Indigofera astragalina", *International Journal of Drug Research and Technology.*, vol 4., bll 46-54., 2014.

[29] S. Srinivasan, W. Wankhar, S. Rathinasamy, en R. Rajan, "Neuroprotective effects of Indigofera tinctoria on noise stress affected Wistar albino rat brain", *Journal of Applied Pharmaceutical Science*, vol 5, no 6, bll 058–065, 2015, doi: 10.7324/JAPS.2015.50609.

[30] B. Madakkannu en R. Ravichandran, "In vivo immunoprotective role of Indigofera tinctoria and Scoparia dulcis aqueous extracts against chronic noise stress induced immune abnormalities in Wistar albino rats", *Toxicology Reports*, vol 4, no March, bll 484–493, 2017, doi: 10.1016/j.toxrep.2017.09.001.

[31] M. A. Hossain *et al.*, "An integrated in-silico Pharmaco-BioInformatics approaches to identify synergistic effects of COVID-19 to HIV patients", *Computers in Biology and Medicine*, vol 155, no September 2022, bl 106656, 2023, doi: 10.1016/j.compbiomed.2023.106656.

[32] F. M. Begum SM, Z. Fathima S, P. S, S. R, en H. S, "Screening Indian Medicinal Plants to Control Diabetes – An In silico and In vitro Approach", *General Medicine: Open Access*, vol 05, no 02, 2017, doi: 10.4172/2327-5146.1000289.

[33] and R. S. S. Tharaheswari M., Kumar J. S. P., Reddy N. J., Subhashree S., "Fenugreek Seed Extract Stabilize Plasma Lipid Levels in Type 2 Diabetes by Modulating PPARs and GLUT4 in Insulin Target Tissues 18.", *Am. J. Phytomedicine Clin. Ther.*, vol 2, no, bll 587–602, 2014.

[34] R. L. Frkic *et al.*, "PPARγ in Complex with an Antagonist and Inverse Agonist: a Tumble and Trap Mechanism of the Activation Helix", *iScience*, vol 5, bll 69–79, 2018, doi: 10.1016/j.isci.2018.06.012.

[35] T. H. Chen, M. J. Tsai, Y. S. Fu, en C. F. Weng, "The exploration of natural compounds for anti-diabetes from distinctive species Garcinia linii with comprehensive review of the garcinia family", *Biomolecules*, vol 9, no 11, 2019, doi: 10.3390/biom9110641.

[36] G. Brusotti *et al.*, "Betulinic acid is a PPARλ antagonist that improves glucose uptake, promotes osteogenesis and inhibits adipogenesis", *Scientific Reports*, vol 7, no 1, bl 5777, 2017, doi: 10.1038/s41598-017-05666-6.

[37] S. Kume, T. Uzu, K. Isshiki, en D. Koya, "Peroxisome proliferator-activated receptors in diabetic nephropathy", *PPAR Research*, vol 87952, 2008, doi: 10.1155/2008/879523.

[38] "Protein Data Bank". [Online]. Available at: https://www.rcsb.org/

[39] G. M. Morris *et al.*, "Software news and updates AutoDock4 and AutoDockTools4: Automated docking with selective receptor flexibility", *Journal of Computational Chemistry*, vol 30, no 16, bll 2785–2791, 2009, doi: 10.1002/jcc.21256.

[40] "IMPPAT: Indian Medicinal Plants, Phytochemistry And Therapeutics". [Online]. Available at: https://cb.imsc.res.in/imppat/

[41] "PubChem Dat Bank". [Online]. Available at: https://pubchem.ncbi.nlm.nih.gov/

[42] "BIOVIA, Dassault Systèmes, Discovery Studio , 2021, San Diego: Dassault Systèmes, 2021. - Google Search". [Online]. Available at: https://discover.3ds.com/discovery-studio-visualizer

[43] O. Trott en A. J. Olson, "AutoDock Vina: Improving the speed and accuracy of docking with a new scoring function, efficient optimization, and multithreading", *Journal of Computational Chemistry*, vol 31, no 2, 2009, doi: 10.1002/jcc.21334.

[44] G. M. Morris *et al.*, "Automated docking using a Lamarckian genetic algorithm and an empirical binding free energy function", *Journal of Computational Chemistry*, vol 19, no 14, bll 1639–1662, 1998, doi: 10.1002/(SICI)1096-987X(19981115)19:14<1639::AID-JCC10>3.0.CO;2-B.

[45] W. Tian, C. Chen, X. Lei, J. Zhao, en J. Liang, "CASTp 3.0: Computed atlas of surface topography of proteins", *Nucleic Acids Research*, vol 46, no W1, bll W363–W367, 2018, doi: 10.1093/nar/gky473.

[46] "Molinspiration Cheminformatics Publications". Toegang verkry: 23 November 2023. [Online]. Available at: https://www.molinspiration.com/cgi-bin/properties

[47] "SwissADME". Toegang verkry: 24 November 2023. [Online]. Available at: http://www.swissadme.ch/

[48] D. E. V. Pires, T. L. Blundell, en D. B. Ascher, "pkCSM: Predicting small-molecule pharmacokinetic and toxicity properties using graph-based signatures", *Journal of Medicinal Chemistry*, vol 58, no 9, bll 4066–4072, 2015, doi: 10.1021/acs.jmedchem.5b00104.

[49] "ADMETlab 2.0". Toegang verkry: 24 November 2023. [Online]. Available at: https://admetmesh.scbdd.com/

[50] C. A. Lipinski, F. Lombardo, B. W. Dominy, en P. J. Feeney, "Experimental and computational approaches to estimate solubility and permeability in drug discovery and development settings", *Advanced Drug Delivery Reviews*, vol 64, no SUPPL., bll 4–17, 2012, doi: 10.1016/j.addr.2012.09.019.

[51] S. A. Ashraf *et al.*, "Multi-targeted molecular docking, pharmacokinetics, and drug-likeness evaluation of okra-derived ligand abscisic acid targeting signaling proteins involved in the development of diabetes", *Molecules*, vol 26, no 19, Okt 2021, doi: 10.3390/molecules26195957.

[52] W. Luo *et al.*, "Integration of molecular docking, molecular dynamics and network pharmacology to explore the multi-target pharmacology of fenugreek against diabetes", *Journal of Cellular and Molecular Medicine*, vol 27, no 14, bll 1959–1974, Jul 2023, doi: 10.1111/jcmm.17787.

[53] D. B. Savage *et al.*, "Action in Humans", *Diabetes*, vol 50, bll 2199–2202, 2001.

[54] N. K. Salam, T. H. W. Huang, B. P. Kota, M. S. Kim, Y. Li, en D. E. Hibbs, "Novel PPAR-gamma agonists identified from a natural product library: A virtual screening, induced-fit docking and biological assay study", *Chemical Biology and Drug Design*, vol 71, no 1, bll 57–70, 2008, doi: 10.1111/j.1747-0285.2007.00606.x.

[55] J. M. Olefsky en A. R. Saltiel, "PPARγ and the treatment of insulin resistance", *Trends in Endocrinology and Metabolism*, vol 11, no 9, bll 362–368, 2000, doi: 10.1016/S1043-2760(00)00306-4.

[56] B. Staels, "PPAR Agonists and the Metabolic Syndrome", *Therapies*, vol 62, bll 319–326., 2007.

[57] Y. et al. Chandra, V., Huang, P., Hamuro, "Structure of the intact PPAR-γ–RXR-α nuclear receptor complex on DNA", *Nature*, vol 456, bll 350–356, 2008, doi: https://doi.org/10.1038/nature07413.